Radiative heat transfer on optically thick fluid past an oscillating vertical plate with variable temperature

ABSTRACT

A theoretical study on radiation heat transfer with reference to an optically thick fluid past an oscillating vertical flat plate with variable temperature in the presence of convection and radiation has been presented. The fluid is considered to be a gray, absorbing-emitting radiation but non- scattering medium. The Rosseland flux approximation plays an important role in determining the effect of radiation heat transfer contribution. This problem is an improvement of Stoke's first and second problem to justify the physical signifance on this problem. This problem is solved by employing Laplace transfrom method. Numerical results of velocity and temperature distributions are depicted graphically. Also, numerical results of frictional shearing stress and critical Grashof number are presented in tables.

Keywords: Thermal radiation, gray gas flow, Grashof number, Rosseland model, radiative heat-flux.

1. Introduction

Radiation heat transfer of an optically dense medium is subjected to a large optical thickness as defined just as with molecular conductivity the transfer of radiant energy in a medium to compare with diffusion transfer. Here, the interphoton collision becomes predominant. For large optical thickness (optically dense medium), a gray body radiation depends on the basis of diffusion concept of radiation heat transfer. This leads to Rosseland approximation for an optically thick medium. The study of radiation heat transfer of an optically thick fluid has received wide attention to many researchers in the field of engineering and space physics. The importance of a study of thermal radiation effect takes place in a numerious applications of condensed fuel combustion, solar energy collectors, heat exchangers, glass and ceramics manufacture, rocket propulsion chembers and laser processing of materials. A litereture survey reveals to the study of Chen et. al [1], Reddy and Kumar [2], Nassab and Maramisaran [3], Obidina and Kiseleva [4], Saladino and Farmer [5] and Gedda et. al [6]. An account of the problem on radiation convection flows gives rise to include the Schuster-Schwartzchild two flux model,the Milne-Eddington approximation and the Rosseland diffusion flux model (Siegel and Howell [7]). Each flux model has its relative benefits and different regimes of validity. Davies [8] studied the free and forced convection flow on a plate with thermal radiation by employing a heat- balance integral method. Chen et. al [9] studied free gray absorbing -emitting, non-scattering convection boundary layer flow along an isothermal horizontal plate with thermal radiation flux using the Rosseland diffusion model. Chamkha et. al [10] have studied viscoelastic free convection boundary layer flow from a doubly inclined geometry i.e., wedge, in porous media with the Rosseland diffusion flux model. Bestman [11] studied asymptotic compressible flow along a long vertical hot plate in the presence of an externally applied magnetic field with strong radiative transfer and temperature dependent viscosity and thermal conductivity, using differential approximation for the radiative flux. Campo and Schuler [12] investigated numerically the interaction of forced convection and thermal radiation heat transfer in laminar absorbing-emitting gray gas pipe flow using the method of moments to approximate the radiative heat flux. Yih [13] employed the Rosseland flux model to study numerically the radiative effects on free convection boundary layer flow from an isothermal vertical cylinder in porous media. Hossain et. al [14] used the Rosseland diffusion radiation flux model to simulate the natural convection, variable viscosity heat transfer from a vertical plate with suction effects. An oscillating plate temperature effect on a flow past an infinite vertical porous late with constant suction and embedded in a porous medium was examined by Jaiswal and Soundalgekar [15]. Muthucumaraswamy and Ganesan [16] examined the radiation effects on flow past an impulsively started infinite vertical plate with variable temperature. Makinde [17] employed a superposition technique and a Rosseland difffusion flux model to study the natural convection heat and mass transfer in a gray, absorbing- emitting fluid along a porous vertical translating plate. Kumar and Verma [18] examined the thermal radiation and mass transfer effects on an MHD flow past a vertical oscillating plate with variable temperature and mass diffusion. An unsteady radiative flow past an oscillating semi-infinite vertical plate with uniform mass flux was presented by Muthucumaraswamy and Saravanan [19] . Ghosh et al. [20] investigated the transient MHD free convection flow of an optically thick gray gas past a moving vertical plate in the presence of thermal radiation and mass diffusion. An MHD radiating heat/mass transport in a Darcian porous regime bounded by an oscillating vertical surface was presented by Ahmed et al. [21] . Thermal radiation on oscillatory flow past a moving vertical plate in a time varying gravity field has been investigated by Ghosh Swapan Kumar [22]. Nevertheless, several investigations on different aspect of flow have been carried out by Biswas et. al [23], Biswas and Ahmed [24]. Biswas et. al [25 - 26], Ahmed and Biswas [27], Gazi et. al [28] and Ghosh [29 - 30].

The purpose of present investigation is to deal with radiative heat transfer of an optically dense medium with temperature variation along an infinite oscillating vertical flat plate with reference to gravity driven radiation- convection flow. The importance of a study of such fluid flow problem by employing Rosseland diffusion flux model takes place of a gray gas flow by which the fluid is considered to be gray, absorbing - emitting radiation but non- scattering medium. This problem is an improvement of Stoke's first and second problem to generate gravity driven radiation- convection flow. This mathematical study does not seem to appeared in the literature. The importance of a study of this problem lies in its application of fluid engineering, space craft propulsion system and high temperature physics.

2. Formulation of the problem and its solution

consider an unsteady flow of a viscous incompressible fluid occupying a semi-infinite region of space bounded by an infinite vertical flat plate with variable temperature moving with uniform velocity u_0 which varies harmonically with time in the presence of convection and radiation. The fluid is considered to be a gray, absorbing-emitting radiation but non-scattering medium. To choose cartesian co-ordinate system in such a way that x'-axis is taken along the plate and y'-axis is normal to it. It is considered that all fluid properties are constant except the influence of density variation in the body force term. Initally, the plate and fluid are at same temperature in a stationary condition. At time $t' > 0,$ the plate is given an impulsive motion in the vertical direction against the gravitional field with the constant velocity u_0, which varies harmonically with time and the plate temperature is made to rise linearly with time. Since the plate is infinite along x'-direction, all physical quantites are functions of y' and t' only.

Under the Boussinesq approximation, the flow is governed by the following equation

$$\frac{\partial u'}{\partial t'} = \nu \frac{\partial^2 u'}{\partial y'^2} + g\beta\left(T' - T'_\infty\right) \qquad (1)$$

The energy equation becomes

$$\frac{\partial T'}{\partial t'} = \frac{k}{\rho c_p}\frac{\partial^2 T'}{\partial y'^2} - \frac{1}{\rho c_p}\frac{\partial q_r}{\partial y'} \quad (2)$$

where $u', t', \nu, g, \beta, T', T'_\infty, k, c_p, \rho$ and q_r are respectively, the velocity component along the plate, the time, the kinematic coefficient of viscosity, the gravitational acceleration, the coefficient of thermal expansion, the temperature of the fluid, the temperature of the fluid far away from the plate, the thermal conductivity, the specific heat at constant pressure, the density of the fluid and the radiative heat-flux.

The boundary conditions are

$$\begin{aligned} &u' = 0,\ T' = T'_\infty \ \text{ for all } y',\ t' \le 0 \\ &t' > 0 : u' = u_0 \cos\omega' t',\ T' = T'_\infty + \left(T'_w - T'_\infty\right) A t' \ \text{ at } y' = 0 \\ &u' \to 0,\ T' \to T'_\infty \ \text{ as } y' \to \infty \end{aligned} \quad (3)$$

where $A = u_0^2/\nu$, T'_w is the temperature at the plate, u_0 is the velocity of the plate and ω' is the frequency of oscillations.

Introducing dimensionless quantities

$$u = \frac{u'}{u_0},\quad y = \frac{y' u_0}{\nu},\quad t = \frac{t' u_0^2}{\nu},\quad \omega = \frac{\omega' \nu}{u_0{}^2}$$

$$T = \frac{T' - T'_\infty}{T'_w - T'_\infty},\quad \Pr = \frac{\nu}{a} = \frac{\rho \nu c_p}{k} \ \text{ and } \ \mathrm{Gr} = \frac{g\beta\nu\left(T'_w - T'_\infty\right)}{u_0{}^3} \ \text{ is the Grashof number} \quad (4)$$

the equation (1) together with the dimensionless quantities (4) transform into

$$\frac{\partial u}{\partial t} = \frac{\partial^2 u}{\partial y^2} + Gr\,T \quad (5)$$

The radiation flux vector can be found from Isachenko et al. [31] and its formula is derived on the basis of the diffusion concept of radiation heat transfer in the following way:

$$q_r = -\frac{4\sigma}{3k^*}\frac{\partial T'^4}{\partial y'} \quad (6)$$

where σ and k^* are respectively, the Stefan-Boltzman constant and the spectrul mean absorption coefficient of the medium.

It is assumed that the temperature differences within the flow are sufficiently small such that T'^4 may be regarded as a linear function of temperature. It can be established by expanding T'^4 i.e. a Taylor series about T'_∞ and neglecting higher order term. Therefore T'^4 can be expressed in the following way

$$T'^4 = 4T'^3_\infty T' - 3T'^4_\infty \quad (7)$$

Using (6) and (7), equation (2) takes the form

$$\frac{\partial T'}{\partial t'} = \frac{k}{\rho c_p}\frac{\partial^2 T'}{\partial y'^2} + \frac{16\sigma T'^3_\infty}{3k^*}\frac{1}{\rho c_p}\frac{\partial^2 T'}{\partial y'^2} \quad (8)$$

Using dimensionless quantities (4) , the equation (8) can be written in a dimensionless form

$$\left(1 + k_1\right)\frac{\partial^2 T}{\partial y^2} - \Pr\frac{\partial T}{\partial t} = 0 \quad (9)$$

where $k_1 = \dfrac{16\sigma T_\infty^{'3}}{3k^* k}$ is the radiation parameter.

The dimensionless boundary conditions turn into

$$u = 0,\ T = 0 \ \text{ for all } y,\ t \le 0$$

$$t > 0: \ u = \cos\omega t, \ \ T = t \quad \text{at } y = 0 \tag{10}$$
$$u \to 0, \ T \to 0 \ \text{ at } \ y \to \infty$$

Applying Laplace transform of (5) and (9) in the following

$$su^* = \frac{\partial^2 u^*}{\partial y^2} + \mathrm{Gr}T^* \tag{11}$$

$$(1+k_1)\frac{\partial^2 T^*}{\partial y^2} - \Pr s T^* = 0 \tag{12}$$

The corresponding boundary conditions become

$$u^* = 0, \quad T^* = 0 \ \text{ for all } \ y, \ \frac{1}{s^2} \le 0$$
$$\frac{1}{s^2} > 0: \ u^* = \frac{s}{s^2+\omega^2}, \ \ T^* = \frac{1}{s^2} \ \text{ at } \ y = 0 \tag{13}$$
$$u^* \to 0, \ T^* \to 0 \ \text{ at } \ y \to \infty$$

Here, $$u^* = \frac{s}{s^2+\omega^2} = \frac{1}{2}\left[\frac{1}{s+i\omega} + \frac{1}{s-i\omega}\right] \tag{14}$$

By applying temperature boundary conditions given by (13), equation (12) becomes

$$T^* = \frac{1}{s^2} e^{-\sqrt{\frac{\Pr s}{1+k_1}}\, y} \tag{15}$$

Using (15), equation (11) becomes

$$su^* = \frac{\partial^2 u^*}{\partial y^2} + \frac{\mathrm{Gr}}{s^2} e^{-\sqrt{\frac{\Pr s}{1+k_1}}\, y} \tag{16 }$$

By applying Laplace inversion method, the equation (14) gives

$$\mathrm{L}^{-1}\left\{\frac{1}{s+i\omega}\right\} = e^{-i\omega t}, \quad \mathrm{L}^{-1}\left\{\frac{1}{s-i\omega}\right\} = e^{i\omega t}, \ \ \mathrm{L}^{-1}\left\{e^{-\sqrt{s}y}\right\} = \frac{y}{2\sqrt{\pi t^3}} e^{-\frac{y^2}{4t}} \tag{17}$$

Using Convolution theorem with reference to Laplace Inversion method together with the boundary condition (13) subject to (17), the solution of velocity and temperature distribution with reference to (16) and (15) such as

$$\begin{aligned} u(y,t) = \frac{1}{4}\Bigg[& e^{\left(y\sqrt{-i\omega}-i\omega t\right)}\mathrm{erfc}\left(\frac{y}{2\sqrt{t}} + \sqrt{-i\omega t}\right) + e^{-\left(y\sqrt{-i\omega}+i\omega t\right)}\mathrm{erfc}\left(\frac{y}{2\sqrt{t}} - \sqrt{-i\omega t}\right) \\ & + e^{\left(y\sqrt{i\omega}+i\omega t\right)}\mathrm{erfc}\left(\frac{y}{2\sqrt{t}} + \sqrt{i\omega t}\right) + e^{-\left(y\sqrt{i\omega}-i\omega t\right)}\mathrm{erfc}\left(\frac{y}{2\sqrt{t}} - \sqrt{i\omega t}\right)\Bigg] \\ & + \frac{\mathrm{Gr}}{\alpha-1}\left[\left\{\frac{1}{2}\left(t^2+y^2t\right) + \frac{y^4}{24}\right\}\mathrm{erfc}\left(\frac{y}{2\sqrt{t}}\right) - y\sqrt{\frac{t}{\pi}}\left(\frac{5}{6}t + \frac{y^2}{12}\right)e^{-\frac{y^2}{4t}}\right] \\ & - \frac{\mathrm{Gr}}{\alpha-1}\left[\left\{\frac{1}{2}\left(t^2+\alpha y^2 t\right) + \frac{\alpha^2}{24}y^4\right\}\mathrm{erfc}\left(\frac{y\sqrt{\alpha}}{2\sqrt{t}}\right) - y\sqrt{\alpha}\sqrt{\frac{t}{\pi}}\left(\frac{5}{6}t + \frac{y^2\alpha}{12}\right)e^{-\frac{y^2\alpha}{4t}}\right] \end{aligned} \tag{18}$$

where ω and ωt are, respectively, the dimensionless frequency of oscillations and phase angle and

$$T(y,t)=\left(t+\frac{y^2}{2}\alpha\right)\mathrm{erfc}\left(\frac{y}{2}\sqrt{\frac{\alpha}{t}}\right)-y\sqrt{\alpha}\sqrt{\frac{t}{\pi}}\,e^{-\frac{y^2\alpha}{4t}}, \tag{19}$$

where $\alpha=\dfrac{\Pr}{1+k_1}$

Particular case of interest:

Non–oscillatory case by putting $\omega=0$ and $\omega t=0$. The dimensionless boundary conditions (10) turns into

$$\begin{aligned} &u=0,\ T=0 \quad \text{for all} \quad y,\ t\le 0\\ &t>0: u=1,\ \ T=t \ \ \text{at}\ y=0\\ &u\to 0,\ \ T\to 0 \quad \text{as} \quad y\to\infty \end{aligned} \tag{20}$$

By applying Laplace transform subject to equations (11) and (12) together with the boundary condition (20) the velocity and temperature distribution can be obtained by the help of Laplace Inversion method such as

$$\begin{aligned} u(y,t)=\mathrm{erfc}\left(\frac{y}{2\sqrt{t}}\right)&+\frac{\mathrm{Gr}}{\alpha-1}\left[\left\{\frac{1}{2}\left(t^2+y^2t\right)+\frac{y^4}{24}\right\}\mathrm{erfc}\left(\frac{y}{2\sqrt{t}}\right)-y\sqrt{\frac{t}{\pi}}\left(\frac{5}{6}t+\frac{y^2}{12}\right)e^{-\frac{y^2}{4t}}\right]\\ &-\frac{\mathrm{Gr}}{\alpha-1}\left[\left\{\frac{1}{2}\left(t^2+\alpha y^2t\right)+\frac{\alpha^2y^4}{24}\right\}\mathrm{erfc}\left(\frac{y\sqrt{\alpha}}{2\sqrt{t}}\right)-y\sqrt{\alpha}\sqrt{\frac{t}{\pi}}\left(\frac{5}{6}t+\frac{y^2\alpha}{12}\right)e^{-\frac{y^2\alpha}{4t}}\right] \end{aligned} \tag{21a}$$

$$T(y,t)=\left(t+\frac{y^2}{2}\alpha\right)\mathrm{erfc}\left(\frac{y}{2}\sqrt{\frac{\alpha}{t}}\right)-y\sqrt{\alpha}\sqrt{\frac{t}{\pi}}\,e^{-\frac{y^2\alpha}{4t}} \tag{21b}$$

Shear stress at the plate $y=0$ for $\omega=0$ and $\omega t=0$

$$\tau_x=\left.\frac{du}{dy}\right|_{y=0}=-\frac{1}{\sqrt{\pi t}}-\frac{4}{3}\frac{\mathrm{Gr}}{\alpha-1}t\sqrt{\frac{t}{\pi}}+\frac{1}{2}t\sqrt{\frac{t}{\pi}}\frac{\mathrm{Gr}}{\alpha-1}\left(1-\frac{5}{3}\sqrt{\alpha}\right) \tag{22}$$

In the absence of Grashof number $(\mathrm{Gr}=0)$ the velocity distribution $u(y,t)$ given by (21) takes place

$$u(y,t)=\mathrm{erfc}\left(\frac{y}{2\sqrt{t}}\right) \tag{23}$$

Equation (23) gives the velocity of Stoke's first problem where

$$u(y,t)=\mathrm{erfc}\left(\frac{y}{2\sqrt{t}}\right)=1-\mathrm{erf}\left(\frac{y}{2\sqrt{t}}\right)$$

The temperature distribution (19) gives the Nusselt number Nu at the plate

$$Nu=-\left.\frac{dT}{dy}\right|_{y=0}=2\sqrt{\frac{t}{\pi}}\sqrt{\frac{\Pr}{1+k_1}} \tag{24}$$

3. Results and discussions

The graphical discussions in relevance to the physical interpretation has been made with arbitrary values of radiation parameter (k_1), Grashof number (Gr), Prandtl number ($\Pr$), frequency parameter (ω), phase angle (ωt) and time (t) in Figures 1 to 7. In Figure 1. It is evident that the buoyancy force (Gr) on velocity field leads to increase the flow behavior with increase in Grashof number Gr. As the buoyancy effects become relatively large due to increasing value of Gr, the fluid velocity increases, reaching its peak value near the plate surface and then decreases monotonically to the zero-free stream value satisfying the far field condition. In the case of higher buoyancy it is important to note that there is no flow reversal on velocity field and the maximum peak of the profile occurs at the plate $y=0$ while the peak of the profile decreases steadily near the plate surface. This situation happens in the case of an oscillating plate so that the flow velocity is charactarised by the higher buoyancy to increase the fluid velocity with an increase in Gr. It is noticed from Figure 2. that the fluid velocity decreases with an increase of phase angle (ωt). This situation reavels that the phase angle (ωt) leads to fall the flow velocity on increasing ωt with reference to impulsive onset of the motion. There arises a phase lag on molecular diffusion region with interphoton collision. Figure 3. shows that for buoyancy added flow $(\mathrm{Gr}>0)$ the velocity increases with increase in time (t). The maximum peak of the velocity profiles occurs adjacent to the plate whereas the peak of the profiles quickly decreases on the plate surface. Since the plate oscillates harmonically with time, the velocity profiles are skewed near the plate surface. The skewness is characterised by the impulsive movement of the plate with time variation at the plate. It is observed from Figure 4. that in the absence of oscillation $(\omega=0 \text{ and } \omega t=0)$ and the buoyancy force $(\mathrm{Gr}=0)$, this represents Stoke's flow with reference to the velocity distribution $u(y,t)=\mathrm{erfc}\left(\frac{y}{2\sqrt{t}}\right)=1-\mathrm{erf}\left(\frac{y}{2\sqrt{t}}\right)$. This situation reveals that the velocity increases with increase in time t . Figure 5. reveals that the temperature field (T) increases with an increase in radiation parameter (k_1). Larger values of radiation parameter (k_1) exert its influence on Rosseland approximation in the determination of an increased dominance of thermal radiation over conduction. As such thermal radiation supplements the thermal diffusion and increases the overall thermal diffusivity of the regime since the local radiant diffusion flux model adds radiation conductivity to the conventional thermal conductivity. As a result, the fluid temperature and velocity in the fluid regime of flow are increased. Figure 6. demontrates that with the increase in Prandtl number (Pr) the temperature field (T) decreases near the plate. This is true since; in general, fluid with low Prandtl number has higher thermal conductivity. The higher thermal conductivity means fluid has affinity for heat and so low Prandtl fluid attains comparatively higher temperature. The effect of Prandtl number plays a significant role on diffusion concept of flow medium. If Prandtl number is greater than one ($\mathrm{Pr}>1$) the diffisivity of the flow medium tends to ionization of the flow. In a highly ionized fluid $\mathrm{Pr}>1$, the effect of Prandtl number (Pr = 0.72) for air transformed into ionized state to water. Figure 7. reveals that with an increase in t, there is a strong acceleration in the flow. It is stated that the temperature field (T) increases with an increase in time (t). Thus, time variation at the plate gives rise to increase in temperature with an increase in time (t).

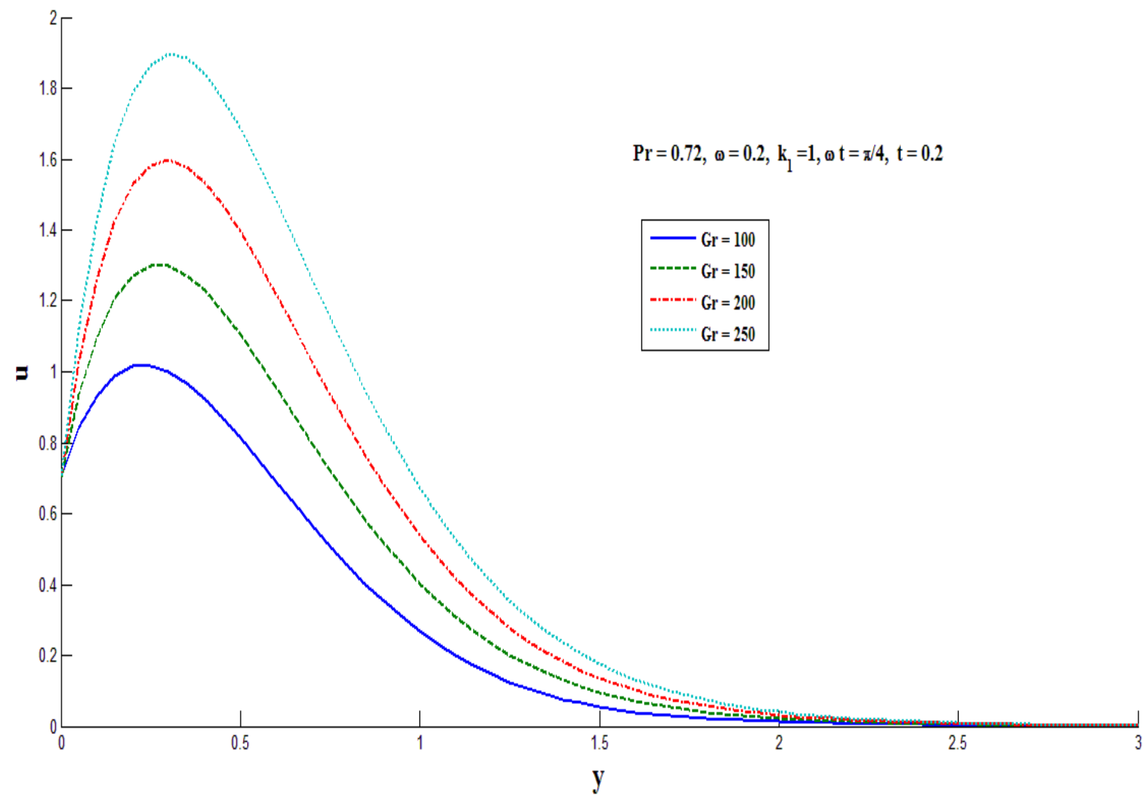

Figure 1. Velocity profiles for large Grashof number Gr

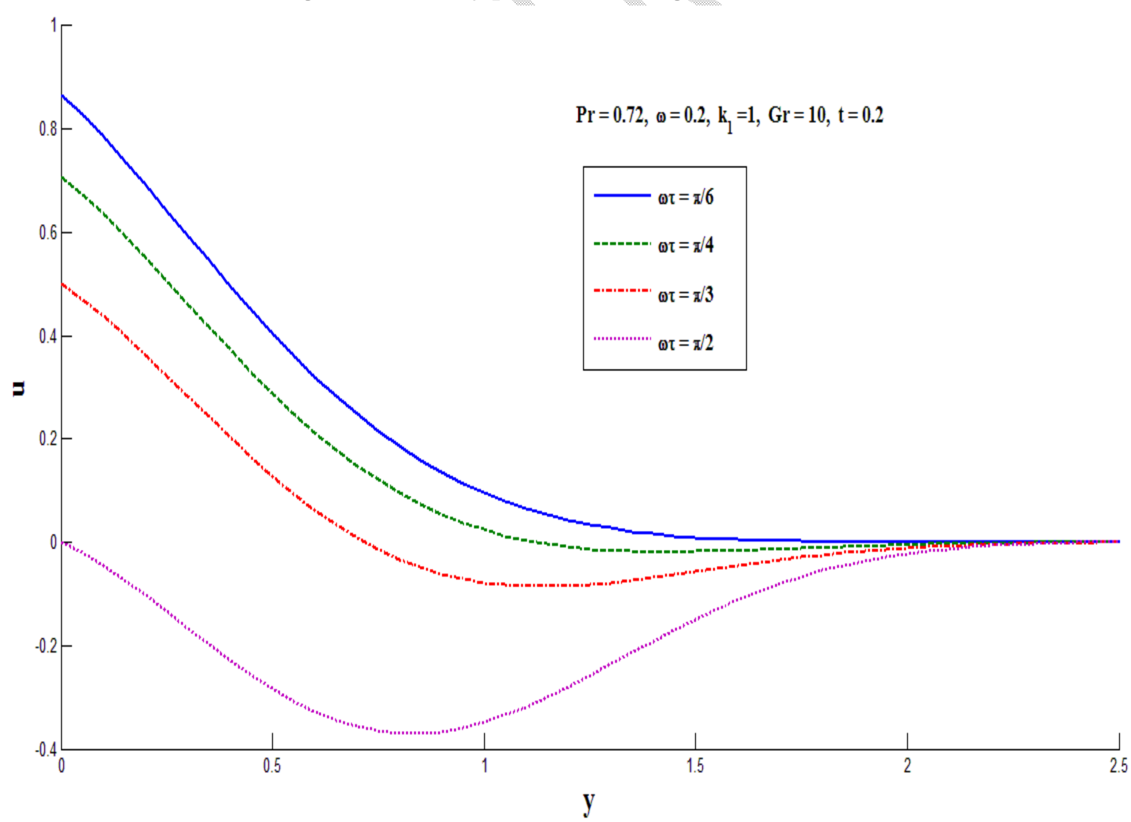

Figure 2. Velocity profiles for increasing ωt

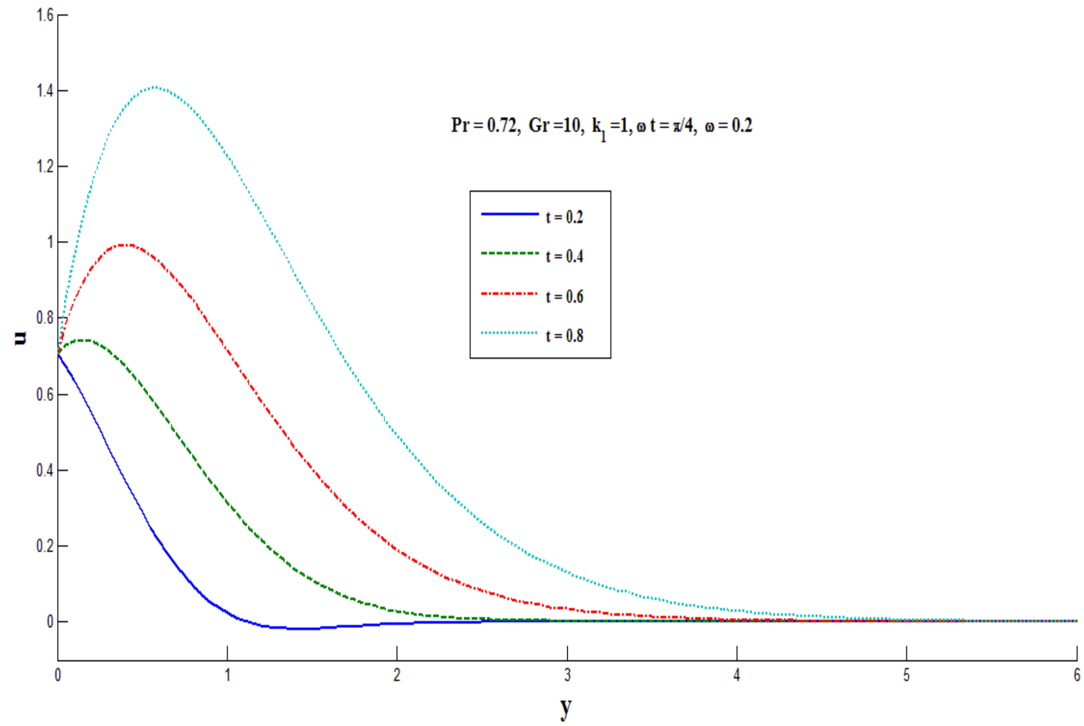

Figure 3. Velocity profiles for increasing time t

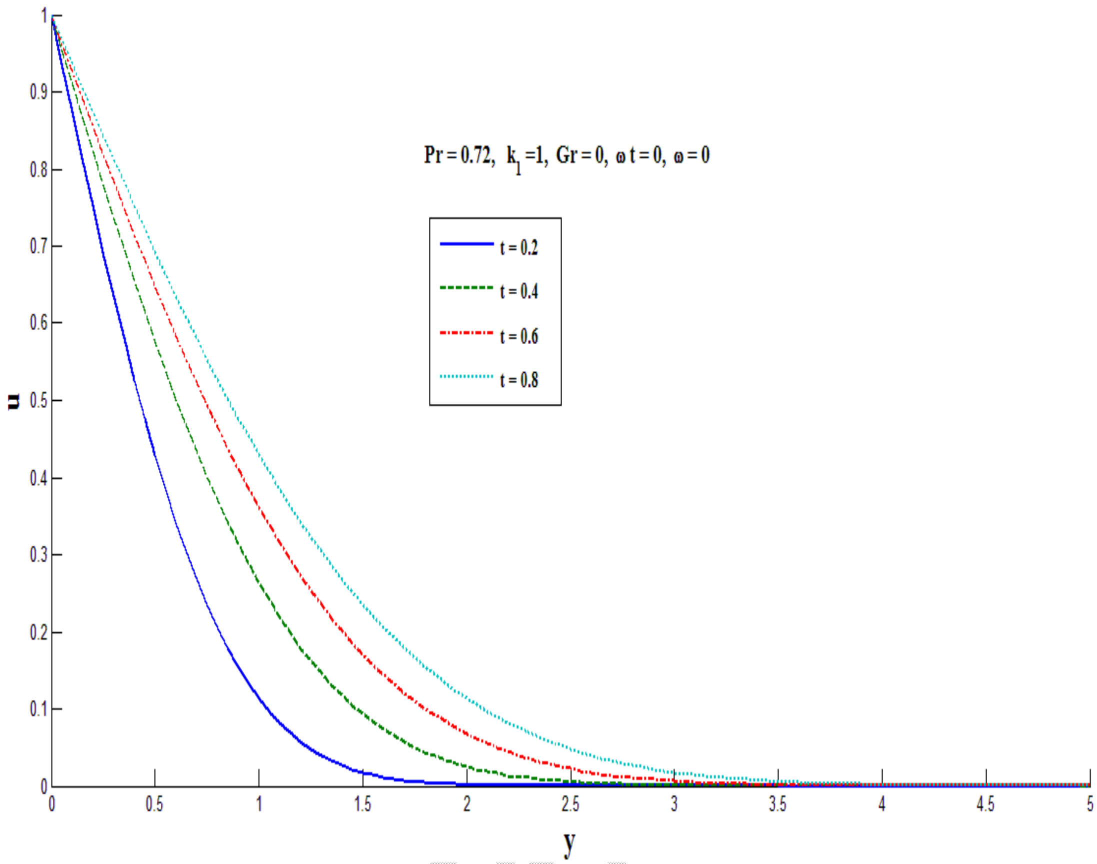

Figure 4. Velocity profiles for increasing time t

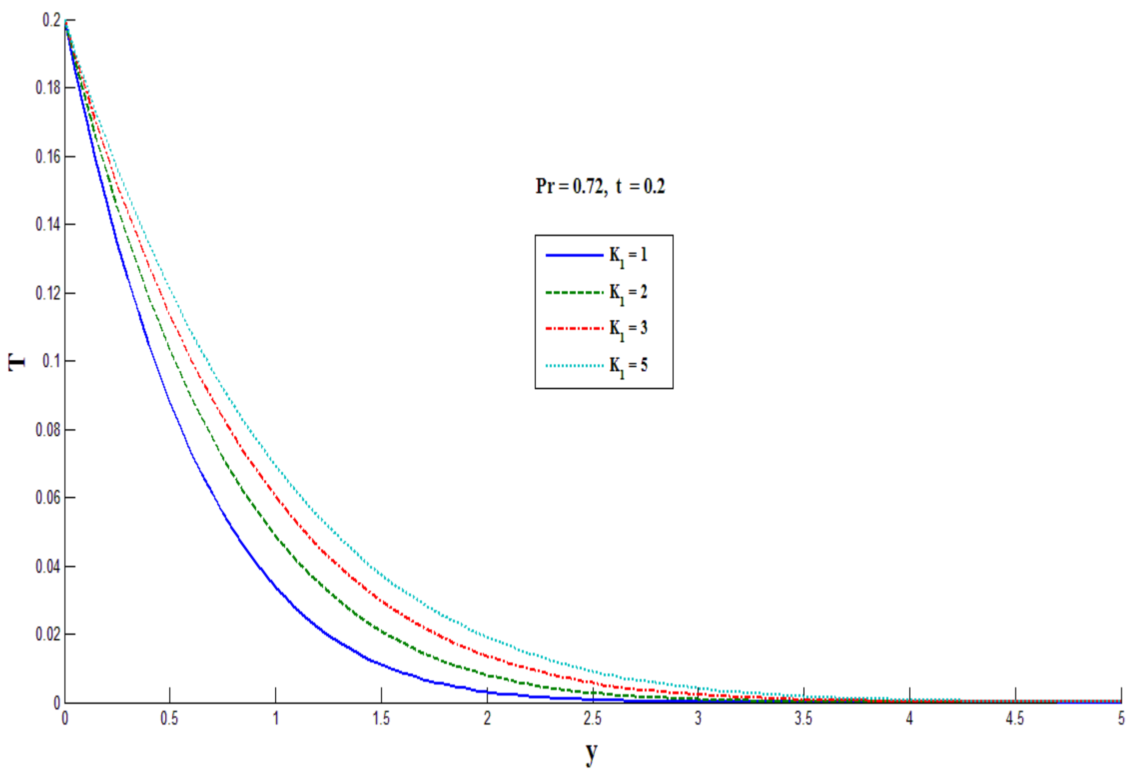

Figure 5. Temperature profiles for increasing k_1

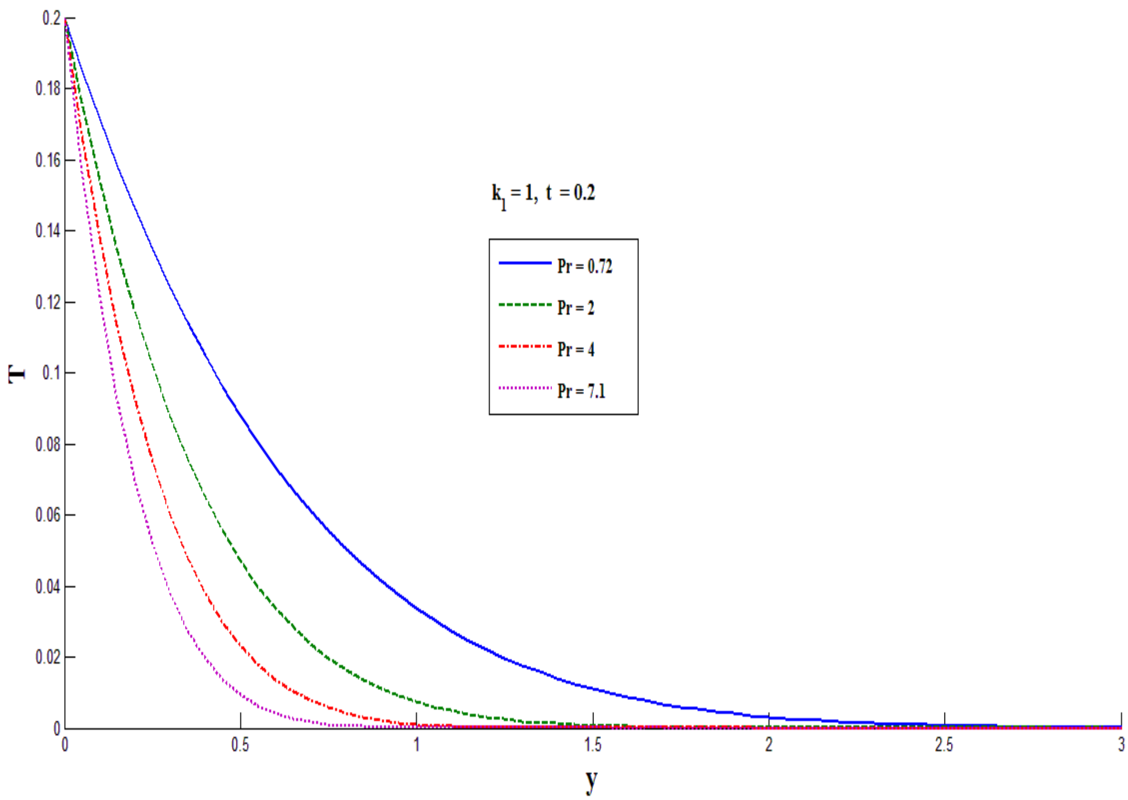

Figure 6. Temperature profiles for increasing Pr

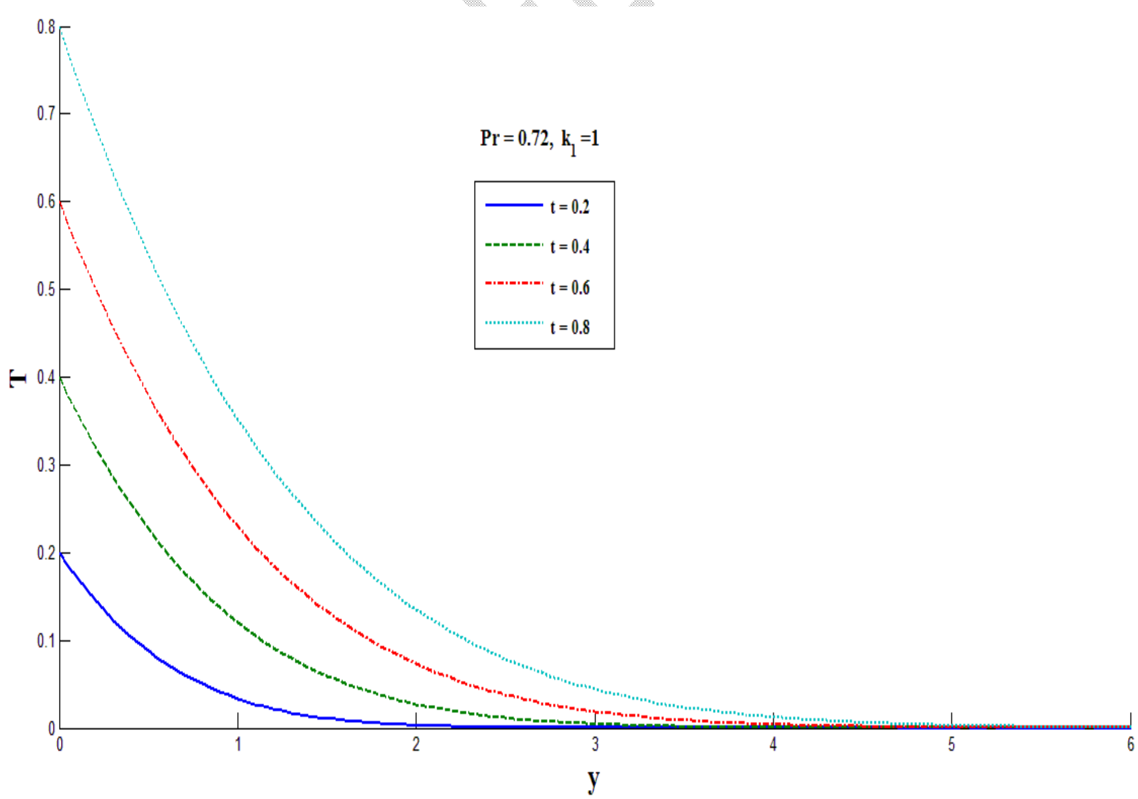

Figure 7. Temperature profiles for increasing time t

Frictional shear stress at the plate $y = 0$:

Frictional shearing stress at the plate can be obtained from $\left.\frac{du}{dy}\right|_{y=0} = 0$ with reference to the solution $u(y,t)$ of (18)

$$\tau_x = \left.\frac{du}{dy}\right|_{y=0}$$

$$= \frac{1}{4}\left[-\frac{2}{\sqrt{\pi t}} + \sqrt{-i\omega}\, e^{-i\omega t} \left\{ \operatorname{erfc}\left(\sqrt{-i\omega t}\right) - \operatorname{erfc}\left(-\sqrt{-i\omega t}\right) \right\} \right.$$

$$\left. -\frac{2}{\sqrt{\pi t}} + \sqrt{i\omega} e^{i\omega t} \left\{ \operatorname{erfc}\left(\sqrt{i\omega t}\right) - \operatorname{erfc}\left(-\sqrt{i\omega t}\right) \right\} \right] + \frac{5}{6}\frac{\text{Gr}}{\alpha - 1}\; t\sqrt{\frac{t}{\pi}}\left(\sqrt{\alpha} - 1\right) \qquad (25)$$

Critical Grashof Number:

Critical Grashof Number can be obtained by putting $\left.\frac{du}{dy}\right|_{y=0} = 0$ in equation (25)

$$\text{Gr}_{\text{crit}} = \frac{1}{A\sqrt{\pi t}} - \frac{1}{4A}\left[\sqrt{-i\omega}\; e^{-i\omega t} \left\{ \operatorname{erfc}\left(\sqrt{-i\omega t}\right) - \operatorname{erfc}\left(-\sqrt{-i\omega t}\right) \right\} \right.$$

$$\left. + \sqrt{i\omega}\; e^{i\omega t} \left\{ \operatorname{erfc}\left(\sqrt{i\omega t}\right) - \operatorname{erfc}\left(-\sqrt{i\omega t}\right) \right\} \right] \qquad (26)$$

where $A = \frac{5}{6}\frac{1}{\alpha - 1} t\sqrt{\frac{t}{\pi}}\left(\sqrt{\alpha} - 1\right)$

Nusselt number Nu at the plate becomes

$$2\sqrt{\frac{\alpha t}{\pi}} \qquad (27)$$

Numerical results of shear stress and critical Grashof number are presented in tables. Table 1 shows that the frictional shear stress at the plate increases with an increase in either radiation parameter (k_1) or time variation (*t*). Also there exist seperation at the plate for $t > 0.2$. Also, frictional drag increases to impede thermal diffusion at the plate surface. Table 2 demonstrates that the frictional shear stress decrease in magnitude with increase in either Grashof number (Gr) or radiation parameter (k_1). This implicates the situation of drag reducing effect to produce stronger thermal diffusion at the plate surface. It is noticed from Table 3 that the frictional shear stress increases with an increase in either phase angle (ωt) or time (*t*). It is interesting to note that there exists separation when $t > 0.4$. Since phase angle rotates about the time variation at the plate the frictional drag is increased to show the influence of thermal radiation at the plate surface. It is evident from Table 4 that there arises a destabilizing influence on the flow field on increasing either radiation parameter (k_1). Table 5 indicates that the Critical Grashof number $(\text{Gr}_{\text{crit}})$ decreases with increase in either phase angle (ωt) or time (*t*) to show the influence of destabilizing effect on the flow field. It is noticed from Tables 4 and 5 that no flow reversal occurs at the plate surface.

Table 1: Shear stress at the plate τ_x for $\text{Pr} = 0.72,\ \text{Gr} = 10,\ \omega = 0.2$ and $\omega t = \frac{\pi}{4}$

t/k_1	1.0	2.0	3.0	4.0	5.0
0.2	– 0.78045	– 0.76103	– 0.76802	– 0.73844	– 0.73095
0.4	0.06960	0.12454	0.16132	0.18844	0.20961
0.6	0.85560	0.95652	1.02411	1.07392	1.11282
0.8	1.69011	1.84549	1.94954	2.02623	2.08612
1.0	2.59257	2.80973	2.95515	3.06233	3.14602

Table 2: Shear stress at the plate τ_x for $\Pr = 0.72$, $\omega = 0.2$, $\omega t = \frac{\pi}{4}$ and $t = 0.2$

Gr/k_1	5.0	10.0	15.0	20.0	25.0
1.0	– 0.91187	– 0.78045	– 0.64905	– 0.51763	– 0.38621
2.0	– 0.90216	– 0.76103	– 0.61991	– 0.47878	– 0.33766
3.0	– 0.89565	– 0.74802	– 0.60040	– 0.45277	– 0.30514
4.0	– 0.89086	– 0.73844	– 0.58602	– 0.43360	– 0.28117
5.0	– 0.88712	– 0.73095	– 0.57479	– 0.41862	– 0.26246

Table 3: Shear stress at the plate τ_x for $\Pr = 0.72$, $\omega = 0.2$, $\mathrm{Gr} = 10$ and $k_1 = 1$

$t/\omega t$	0.0	$\pi/6$	$\pi/4$	$\pi/3$	$\pi/2$
0.2	– 0.99874	– 0.78045	– 0.78045	– 0.68115	– 0.50544
0.4	– 0.14867	– 0.76103	0.06960	0.16890	0.34462
0.6	0.63731	0.76096	0.85560	0.95490	1.13062
0.8	1.47182	1.59547	1.69011	1.78941	1.96512
1.0	2.37429	2.49794	2.59257	2.69188	2.86759

Table 4: Critical Grashof number $\mathrm{Gr}_{\mathrm{crit}}$ for $\Pr = 0.72$, $\omega = 0.2$ and $\omega t = \frac{\pi}{4}$

t/k_1	1.0	2.0	3.0	4.0	5.0
0.2	39.69485	36.96329	35.33497	34.22374	33.40347
0.4	9.06368	8.43998	8.06817	7.81444	7.62715
0.6	3.73500	3.47798	3.32477	3.22021	3.14303
0.8	1.96185	1.82685	1.74637	1.69145	1.65091
1.0	1.17716	1.09615	1.04787	1.01491	0.99059

Table 5: Critical Grashof number $\mathrm{Gr}_{\mathrm{crit}}$ for $\Pr = 0.72$, $k_1 = 1.0$ and $\omega = 0.2$

$t/\omega t$	0^0	$\pi/6$	$\pi/4$	$\pi/3$	$\pi/2$
0.2	48.00001	43.29557	39.69485	35.91665	29.23097
0.4	12.00000	10.33673	9.06368	7.72789	5.36414
0.6	5.33333	4.42796	3.73500	3.00789	1.72123
0.8	3.00000	2.41194	1.96185	1.48958	0.65387
1.0	1.92000	1.49922	1.17716	0.83923	0.24124

4. Conclusion

Radiation heat transfer aspect on transient gray gas flow of an optically thick fluid past an oscillating vertical flat plate variable temperature in the presence of thermal radiation has been presented. This problem is an improvement of Stoke's first and second problem with Rosseland radiation – conduction parameter. The present problem deals with optically dense medium with a decisive importance to black body radiation. The governing equations have been solved by using Laplace transform method. Based on the graphical presentations; the following conclusions can be summarized as follows:

- The velocity profiles are influenced by the Rosseland radiation – conduction parameter.
- The fluid velocity greatly increases for increasing values of Grashof number.
- The fluid velocity is accelerated when time progresses.
- The fluid temperature rises due to increasing radiation parameter or time while it falls for increasing values of Prandtl number.
- The frictional shear stress at the plate is reduced in magnitude with increase in Grashof number or radiation parameter while it is enhanced for increasing values of phase angle.
- The critical Grashof number increases for increasing values of phase angle or time whereas it decreases for increasing values of radiation parameter.

References

1. Chen S L, Ma H K, Chen DY. (1993). Radiation blockage by the interaction of thermal radiation with conduction and convection in the conbustion of the condensed fuel, Int. Commun. Heat and Mass Transfer. 20: 145-157.

2. Reddy KS, Kumar N S. (2008).Combined laminar natural convection and surface radiation heat transfer in a modified cavity receiver of solar parabolic dish, Int. J. Thermal Sci. 47: 1647-1657.

3. Nassab SAG, Maramisaran M. (2009). Transient numerical analysis of a multi layered porous heat exchanger including gas radiation effects, Int. J. Thermal Sci. 48: 1586-1595

4. Obidina SP, Kiseleva MN. (1980). Production of glass with high radiation absorption in the range 0.9–1.2 μm , Glass and Ceramics. 37: 376-378

5. Saladino AJ, Farmer RC. (1993). Radiation/Convection coupling in rocket motor and plume analysis, Final report, SECA Inc., Huntsville, Alabama, USA.

6. Gedda H, Powell J, Wahlstrom G, Li WB, Engstrom H, Magnusson C. (2002) . Energy redistribution during CO_2 laser cladding, J. Laser Appli. 14: 78-82.

7. Siegel R, Howell JR. (1972). Thermal radiation Hear Transfer, Student edition, Mac Graw Hill, 1972.

8. Davies TW. (1995). The cooling of a plate by combined thermal radiation and convection, Int. Commun. Heat Mass Transfer. 12: 405-415.

9. Chen TS, Ali AA, Armaly BF. (1984). Natural convection radiation interaction in boundary layer flow over horizontal surface, AIAA J. 22 (12): 1797-1803

10. Chamkha AJ, Takhar HS, Beg OA. (2004). Radiative free convective non-Newtonian fluid flow past a wedge embedded in a porous medium, Int. J. Fluid Mech. Res. 31 (2): 1-15.

11. Bestman AR. (1985). Compressibility effect on laminar convection to a radiating gas past a vertical plate, Z. Angew, Math. Phys. 36 (5): 767-774.

12. Compo A, Schuler C. (1988). Thermal radiation and laminar forced convection in a gas pipe flow, Heat Mass Transfer 22 (5): 251-257.

13. Yih KA. (1999). Radiation effect on natural convection over a vertical cylinder embedded in a porous media, Int. Commum. Heat and Mass Transfer. 26: 259-267.

14. Hossain MA, Khanafer K, Vafai K. (2001). The effect of radiation on free convection flow of fluid with variable viscosity from a porous vertical plate, Int. J. Thermal Sci. 40: 115-124

15. Jaiswal BS, Soundalgekar VM. (2001). Oscillating plate temperature effects on a flow past an infinite vertical porous late with constant suction and embedded in a porous medium, Heat and Mass Transfer. 37: 125-131.

16. Muthucumaraswamy R, Ganesan P. (2003). Radiation effects on flow past an impulsively started infinite vertical plate with variable temperature, Int. J. Appl. Mech. Eng. 8(1): 125-129.

17. Makinde OD (2005), Free convection flow with thermal radiation and mass transfer past a moving vertical porous plate, Int. Commun. Heat and Mass Transfer. 32: 1411-1419.

18. Kumar AGV, Verma SVK. (2011). Thermal radiation and mass transfer effects on MHD flow past a vertical oscillating plate with variable temperature effects variable mass diffusion, Int. J. Eng. 3: 493–499.

19. Muthucumaraswamy R, Saravanan B. (2013) Numerical solution of unsteady radiative flow past an oscillating semi-infinite vertical plate with uniform mass flux, Comp. Methods in Sci. Tech. 19(1), 1- 9.

20. Ghosh SK, Das S, Jana RN (2015), Transient MHD free convection flow of an optically thick gray gas past a moving vertical plate in the presence of thermal radiation and mass diffusion, J. Appl. Fluid Mech. 8: 65-73.

21. Ahmed S, Batin A, Chamkha AJ. (2015), Numerical/Laplace transform analysis for MHD radiating heat/mass transport in a Darcian porous regime bounded by an oscillating vertical surface, Alexandria Eng. J. 54: 45 - 54.

22. Ghosh Swapan Kumar (2020), Thermal radiation on oscillatory flow past a moving vertical plate in a time varying gravity field, Global journal of engineering and technology advances, 2(1), 001 – 007.

23. Biswas, R., Hossain, M.S, M. Afikuzzaman, and Ahmmed S.F. (2022), "Computational treatment of MHD Maxwell nanofluid flow across a stretching sheet considering higher-order chemical reaction and thermal radiation", *Journal of Computational Mathematics and Data Science*, Volume 4, 100048 (Elsevier)

24. Biswas, R. and Ahmmed, S. F. (2018), "Effects of Hall current and chemical reaction on MHD unsteady heat and mass transfer of Casson nanofluid flow through a vertical plate", *Journal of Heat Transfer(ASME)*, 140/ 092402-1.

25. Biswas, R. Afikuzzaman, M., Mondal and Ahmmed, S. F. (2018), "MHD free convection and heat transfer flow through a vertical porous plate in the presence of chemical reaction", *Frontiers in Heat and Mass Transfer* (FHMT), 11: 13.

26. Biswas, R., Mondal, M. and Islam, A. (2019), "A steady MHD natural convection heat transfer fluid flow through a vertical surface in the existence of Hall current and radiation", *Instrumentation, Mesure, Métrologie*. 2: 331-356.

27. Ahmmed, S. F. and **Biswas, R.** (2019), "Effects of radiation and chemical reaction on MHD unsteady heat and mass transfer of nanofluid flow through a vertical plate", *Modelling Measurement and Control B*. 87(4): 213-220.

28. Gazi, M.A., Suma, U. K., Katun, M., Md. Taibur Rahaman, Sarder Firoz Ahmmed, and **Biswas**, **R.** **(**2022), "A Numerical Evolution of MHD Maxwell Fluid Flow through an Isothermal Radiated Stretching Sheet with Higher Order Chemical Reaction", *Asian Journal of Pure and Applied Mathematics*, 4(3), 329-353.

29. Ghosh, S K (2022), A new investigation on resonance of the Sun with a decisive importance to magnetohydrodynamic (MHD) pure shear flow permeated by an oblique magnetic field, Journal of energy research and reviews,12 (2), 14 – 25.

30. Ghosh, S K (2022), Temperature dependence on transient hydrodynamic gravity driven flow down an inclined plane, Journal of energy research and reviews, 12 (3), 16 – 25.

31. Isachenko VP, Osipova VA. Sukomel AS (1980), Heat Transfer, Mir Publishers, Moscow, USSR

.

.